

Search for Excited Leptons in e^+e^- Collisions at $\sqrt{s} = 161$ GeV

The OPAL Collaboration

Abstract

We have searched for excited states of charged and neutral leptons, e^* , μ^* , τ^* and ν^* , in e^+e^- collisions at $\sqrt{s} = 161$ GeV using the OPAL detector at LEP. No evidence for their existence was found. With the most common coupling assumptions, the topologies from excited lepton pair production include $\ell^+\ell^-\gamma\gamma$ and $\ell^+\ell^-W^+W^-$, with the subsequent decay of the virtual W bosons. From the analysis of these topologies, 95% confidence level lower mass limits of 79.9 GeV for e^* , 80.0 GeV for μ^* , 79.1 GeV for τ^* , 78.3 GeV for ν_e^* , 78.9 GeV for ν_μ^* and 76.2 GeV for ν_τ^* are inferred. From the analysis of W^+W^- and $\gamma\gamma$ topologies with missing energy and using alternative coupling assignments which favour charged $\ell^{*\pm}$ and photonic ν^* decays, 95% confidence level lower mass limits of 77.1 GeV for each $\ell^{*\pm}$ flavour and 77.8 GeV for each ν^* flavour are inferred. From the analysis of the $\ell^+\ell^-\gamma$, $\ell^\pm W^\mp$ and single γ final states expected from excited lepton single production, upper limits on the ratio of the coupling to the compositeness scale, f/Λ , are determined for excited lepton masses up to the kinematic limit.

Submitted to Physics Letters B

The OPAL Collaboration

K. Ackerstaff⁸, G. Alexander²³, J. Allison¹⁶, N. Altekamp⁵, K. Ametewee²⁵, K.J. Anderson⁹, S. Anderson¹², S. Arcelli², S. Asai²⁴, D. Axen²⁹, G. Azuelos^{18,a}, A.H. Ball¹⁷, E. Barberio⁸, R.J. Barlow¹⁶, R. Bartoldus³, J.R. Batley⁵, J. Bechtluft¹⁴, C. Beeston¹⁶, T. Behnke⁸, A.N. Bell¹, K.W. Bell²⁰, G. Bella²³, S. Bentvelsen⁸, P. Berlich¹⁰, S. Bethke¹⁴, O. Biebel¹⁴, V. Blobel²⁷, I.J. Bloodworth¹, J.E. Bloomer¹, M. Bobinski¹⁰, P. Bock¹¹, H.M. Bosch¹¹, M. Boutemour³⁴, B.T. Bouwens¹², S. Braibant¹², R.M. Brown²⁰, H.J. Burckhart⁸, C. Burgard⁸, R. Bürgin¹⁰, P. Capiluppi², R.K. Carnegie⁶, A.A. Carter¹³, J.R. Carter⁵, C.Y. Chang¹⁷, D.G. Charlton^{1,b}, D. Chrisman⁴, P.E.L. Clarke¹⁵, I. Cohen²³, J.E. Conboy¹⁵, O.C. Cooke¹⁶, M. Cuffiani², S. Dado²², C. Dallapiccola¹⁷, G.M. Dallavalle², S. De Jong¹², L.A. del Pozo⁸, K. Desch³, M.S. Dixit⁷, E. do Couto e Silva¹², M. Doucet¹⁸, E. Duchovni²⁶, G. Duckeck³⁴, I.P. Duerdoth¹⁶, J.E.G. Edwards¹⁶, P.G. Estabrooks⁶, H.G. Evans⁹, M. Evans¹³, F. Fabbrì², P. Fath¹¹, F. Fiedler²⁷, M. Fierro², H.M. Fischer³, R. Folman²⁶, D.G. Fong¹⁷, M. Foucher¹⁷, A. Fürtjes⁸, P. Gagnon⁷, J.W. Gary⁴, J. Gascon¹⁸, S.M. Gascon-Shotkin¹⁷, N.I. Geddes²⁰, C. Geich-Gimbel³, T. Gerasis²⁰, G. Giacomelli², P. Giacomelli⁴, R. Giacomelli², V. Gibson⁵, W.R. Gibson¹³, D.M. Gingrich^{30,a}, D. Glenzinski⁹, J. Goldberg²², M.J. Goodrick⁵, W. Gorn⁴, C. Grandi², E. Gross²⁶, J. Grunhaus²³, M. Gruwé⁸, C. Hajdu³², G.G. Hanson¹², M. Hansroul⁸, M. Hapke¹³, C.K. Hargrove⁷, P.A. Hart⁹, C. Hartmann³, M. Hauschild⁸, C.M. Hawkes⁵, R. Hawkings⁸, R.J. Hemingway⁶, M. Herndon¹⁷, G. Herten¹⁰, R.D. Heuer⁸, M.D. Hildreth⁸, J.C. Hill⁵, S.J. Hillier¹, T. Hilse¹⁰, P.R. Hobson²⁵, R.J. Homer¹, A.K. Honma^{28,a}, D. Horváth^{32,c}, R. Howard²⁹, R.E. Hughes-Jones¹⁶, D.E. Hutchcroft⁵, P. Igo-Kemenes¹¹, D.C. Imrie²⁵, M.R. Ingram¹⁶, K. Ishii²⁴, A. Jawahery¹⁷, P.W. Jeffreys²⁰, H. Jeremie¹⁸, M. Jimack¹, A. Joly¹⁸, C.R. Jones⁵, G. Jones¹⁶, M. Jones⁶, R.W.L. Jones⁸, U. Jost¹¹, P. Jovanovic¹, T.R. Junk⁸, D. Karlen⁶, K. Kawagoe²⁴, T. Kawamoto²⁴, R.K. Keeler²⁸, R.G. Kellogg¹⁷, B.W. Kennedy²⁰, B.J. King⁸, J. Kirk²⁹, S. Kluth⁸, T. Kobayashi²⁴, M. Kobel¹⁰, D.S. Koetke⁶, T.P. Kokott³, M. Kolrep¹⁰, S. Komamiya²⁴, T. Kress¹¹, P. Krieger⁶, J. von Krogh¹¹, P. Kyberd¹³, G.D. Lafferty¹⁶, R. Lahmann¹⁷, W.P. Lai¹⁹, D. Lanske¹⁴, J. Lauber¹⁵, S.R. Lautenschlager³¹, J.G. Layter⁴, D. Lazic²², A.M. Lee³¹, E. Lefebvre¹⁸, D. Lellouch²⁶, J. Letts², L. Levinson²⁶, C. Lewis¹⁵, S.L. Lloyd¹³, F.K. Loebinger¹⁶, G.D. Long¹⁷, M.J. Losty⁷, J. Ludwig¹⁰, M. Mannelli⁸, S. Marcellini², C. Markus³, A.J. Martin¹³, J.P. Martin¹⁸, G. Martinez¹⁷, T. Mashimo²⁴, W. Matthews²⁵, P. Mättig³, W.J. McDonald³⁰, J. McKenna²⁹, E.A. Mckigney¹⁵, T.J. McMahon¹, A.I. McNab¹³, R.A. McPherson⁸, F. Meijers⁸, S. Menke³, F.S. Merritt⁹, H. Mes⁷, J. Meyer²⁷, A. Michelini², G. Mikenberg²⁶, D.J. Miller¹⁵, R. Mir²⁶, W. Mohr¹⁰, A. Montanari², T. Mori²⁴, M. Morii²⁴, U. Müller³, K. Nagai²⁶, I. Nakamura²⁴, H.A. Neal⁸, B. Nellen³, B. Nijhar¹⁶, R. Nisius⁸, S.W. O’Neale¹, F.G. Oakham⁷, F. Odorici², H.O. Ogren¹², N.J. Oldershaw¹⁶, T. Omori²⁴, M.J. Oreglia⁹, S. Orito²⁴, J. Pálinkás^{33,d}, G. Pásztor³², J.R. Pater¹⁶, G.N. Patrick²⁰, J. Patt¹⁰, M.J. Pearce¹, S. Petzold²⁷, P. Pfeifenschneider¹⁴, J.E. Pilcher⁹, J. Pinfold³⁰, D.E. Plane⁸, P. Poffenberger²⁸, B. Poli², A. Posthaus³, H. Przysieznik³⁰, D.L. Rees¹, D. Rigby¹, S. Robertson²⁸, S.A. Robins¹³, N. Rodning³⁰, J.M. Roney²⁸, A. Rooke¹⁵, E. Ros⁸, A.M. Rossi², M. Rosvick²⁸, P. Routenburg³⁰, Y. Rozen²², K. Runge¹⁰, O. Runolfsson⁸, U. Ruppel¹⁴, D.R. Rust¹², R. Rylko²⁵, K. Sachs¹⁰, E.K.G. Sarkisyan²³, M. Sasaki²⁴, C. Sbarra², A.D. Schaile³⁴, O. Schaile³⁴, F. Scharf³, P. Scharff-Hansen⁸, P. Schenk²⁷, B. Schmitt⁸, S. Schmitt¹¹, M. Schröder⁸, H.C. Schultz-Coulon¹⁰, M. Schulz⁸, M. Schumacher³, P. Schütz³, W.G. Scott²⁰, T.G. Shears¹⁶, B.C. Shen⁴, C.H. Shepherd-Themistocleous⁸, P. Sherwood¹⁵, G.P. Siroli², A. Sittler²⁷,

A. Skillman¹⁵, A. Skuja¹⁷, A.M. Smith⁸, T.J. Smith²⁸, G.A. Snow¹⁷, R. Sobie²⁸,
 S. Söldner-Rembold¹⁰, R.W. Springer³⁰, M. Sproston²⁰, A. Stahl³, M. Steiert¹¹, K. Stephens¹⁶,
 J. Steuerer²⁷, B. Stockhausen³, D. Strom¹⁹, F. Strumia⁸, P. Szymanski²⁰, R. Tafirout¹⁸,
 S.D. Talbot¹, S. Tanaka²⁴, P. Taras¹⁸, S. Tarem²², M. Thiergen¹⁰, M.A. Thomson⁸, E. von
 Törne³, S. Towers⁶, I. Trigger¹⁸, T. Tsukamoto²⁴, E. Tsur²³, A.S. Turcot⁹,
 M.F. Turner-Watson⁸, P. Utzat¹¹, R. Van Kooten¹², M. Verzocchi¹⁰, P. Vikas¹⁸, M. Vinciter²⁸,
 E.H. Vokurka¹⁶, F. Wäckerle¹⁰, A. Wagner²⁷, C.P. Ward⁵, D.R. Ward⁵, J.J. Ward¹⁵,
 P.M. Watkins¹, A.T. Watson¹, N.K. Watson⁷, P.S. Wells⁸, N. Wermes³, J.S. White²⁸,
 B. Wilkens¹⁰, G.W. Wilson²⁷, J.A. Wilson¹, G. Wolf²⁶, S. Wotton⁵, T.R. Wyatt¹⁶,
 S. Yamashita²⁴, G. Yekutieli²⁶, V. Zacek¹⁸,

¹School of Physics and Space Research, University of Birmingham, Birmingham B15 2TT, UK

²Dipartimento di Fisica dell' Università di Bologna and INFN, I-40126 Bologna, Italy

³Physikalisches Institut, Universität Bonn, D-53115 Bonn, Germany

⁴Department of Physics, University of California, Riverside CA 92521, USA

⁵Cavendish Laboratory, Cambridge CB3 0HE, UK

⁶Ottawa-Carleton Institute for Physics, Department of Physics, Carleton University, Ottawa, Ontario K1S 5B6, Canada

⁷Centre for Research in Particle Physics, Carleton University, Ottawa, Ontario K1S 5B6, Canada

⁸CERN, European Organisation for Particle Physics, CH-1211 Geneva 23, Switzerland

⁹Enrico Fermi Institute and Department of Physics, University of Chicago, Chicago IL 60637, USA

¹⁰Fakultät für Physik, Albert Ludwigs Universität, D-79104 Freiburg, Germany

¹¹Physikalisches Institut, Universität Heidelberg, D-69120 Heidelberg, Germany

¹²Indiana University, Department of Physics, Swain Hall West 117, Bloomington IN 47405, USA

¹³Queen Mary and Westfield College, University of London, London E1 4NS, UK

¹⁴Technische Hochschule Aachen, III Physikalisches Institut, Sommerfeldstrasse 26-28, D-52056 Aachen, Germany

¹⁵University College London, London WC1E 6BT, UK

¹⁶Department of Physics, Schuster Laboratory, The University, Manchester M13 9PL, UK

¹⁷Department of Physics, University of Maryland, College Park, MD 20742, USA

¹⁸Laboratoire de Physique Nucléaire, Université de Montréal, Montréal, Quebec H3C 3J7, Canada

¹⁹University of Oregon, Department of Physics, Eugene OR 97403, USA

²⁰Rutherford Appleton Laboratory, Chilton, Didcot, Oxfordshire OX11 0QX, UK

²²Department of Physics, Technion-Israel Institute of Technology, Haifa 32000, Israel

²³Department of Physics and Astronomy, Tel Aviv University, Tel Aviv 69978, Israel

²⁴International Centre for Elementary Particle Physics and Department of Physics, University of Tokyo, Tokyo 113, and Kobe University, Kobe 657, Japan

²⁵Brunel University, Uxbridge, Middlesex UB8 3PH, UK

²⁶Particle Physics Department, Weizmann Institute of Science, Rehovot 76100, Israel

²⁷Universität Hamburg/DESY, II Institut für Experimental Physik, Notkestrasse 85, D-22607 Hamburg, Germany

²⁸University of Victoria, Department of Physics, P O Box 3055, Victoria BC V8W 3P6, Canada

²⁹University of British Columbia, Department of Physics, Vancouver BC V6T 1Z1, Canada

³⁰University of Alberta, Department of Physics, Edmonton AB T6G 2J1, Canada

³¹Duke University, Dept of Physics, Durham, NC 27708-0305, USA

³²Research Institute for Particle and Nuclear Physics, H-1525 Budapest, P O Box 49, Hungary

³³Institute of Nuclear Research, H-4001 Debrecen, P O Box 51, Hungary

³⁴Ludwigs-Maximilians-Universität München, Sektion Physik, Am Coulombwall 1, D-85748 Garching, Germany

^a and at TRIUMF, Vancouver, Canada V6T 2A3

^b and Royal Society University Research Fellow

^c and Institute of Nuclear Research, Debrecen, Hungary

^d and Department of Experimental Physics, Lajos Kossuth University, Debrecen, Hungary

1 Introduction

Currently there is no evidence that leptons are composite particles. If the known leptons are bound states of new elementary particles, then excited states, called excited leptons and denoted here as ℓ^* , should exist.¹ Excited leptons have been searched for at the LEP e^+e^- collider at $\sqrt{s} \approx M_Z$ (\sqrt{s} is the centre-of-mass energy) [1, 2] and $\sqrt{s} = 130\text{-}140$ GeV [3, 4] and at the HERA ep collider [5]. Processes such as $e^+e^- \rightarrow \gamma\gamma$ are sensitive to excited particle states at higher mass scales but have less sensitivity than direct searches if direct production is kinematically allowed [6, 7]. In this paper, we describe the OPAL search for excited leptons using 10 pb^{-1} collected during the recent LEP run at $\sqrt{s} = 161$ GeV.

Excited leptons could be produced in pairs in e^+e^- collisions via the process $e^+e^- \rightarrow \ell^*\bar{\ell}^*$, governed by the $\ell^*\bar{\ell}^*V$ coupling, where V is a γ or Z vector boson. The excited leptons are assumed to have the same electroweak $SU(2)$ and $U(1)$ gauge couplings, g and g' , as the Standard Model leptons, but are expected to be grouped in both left- and right-handed weak isodoublets. The existence of the right-handed doublets is required to protect the ordinary light leptons from radiatively acquiring a large anomalous magnetic moment via the $\ell^*\ell V$ interaction [8].

The generators used for excited lepton production are described in Reference [3]. The single production of excited leptons and their decays are governed by the $\ell^*\ell V$ coupling. We use the effective Lagrangian [8]

$$\mathcal{L}\ell\ell^* = \frac{1}{2\Lambda}\bar{\ell}^*\sigma^{\mu\nu}\left[gf\frac{\boldsymbol{\tau}}{2}\mathbf{W}_{\mu\nu} + g'f'\frac{Y}{2}B_\mu\right]\ell + \text{hermitian conjugate}, \quad (1)$$

which describes the generalized magnetic de-excitation of the ℓ^* states. The matrix $\sigma^{\mu\nu}$ is the covariant bilinear tensor, $\boldsymbol{\tau}$ are the Pauli matrices, $\mathbf{W}_{\mu\nu}$ are the electroweak isotriplet vector fields, B_μ is the electroweak singlet field, and Y is the weak hypercharge. The parameter Λ can be regarded as the ‘‘compositeness scale,’’ while f and f' are couplings associated with the different gauge groups.

The three parameters f , f' and Λ in Equation (1) are arbitrary. Different values of the couplings favour different decay modes, and we interpret the search in each experimental topology using coupling assignments that favour that topology. To interpret the results of the searches for photonic decays of charged excited leptons and charged decays of neutral excited leptons, we adopt the coupling convention used in most previous experimental searches, $f = f'$. The model then reduces to one parameter, f/Λ . With this coupling assignment, the branching ratio for $\ell^{*\pm} \rightarrow \ell^\pm\gamma$ varies from essentially 100% for $\ell^{*\pm}$ masses less than the W^\pm mass to about 35% for masses of 160 GeV, and the branching ratio for $\nu^* \rightarrow \ell^\pm W^\mp$ varies from about 80% for ν^* masses less than the W mass to about 65% for masses of 160 GeV. The W may be real or virtual depending on the ν^* mass. The remaining ℓ^* decays are via the Z^0 boson, which are not explicitly considered in this letter.

With the $f = f'$ coupling assignment, photonic ν^* decays are forbidden; there is a complementary assignment, $f = -f'$, for which photonic decays of $\ell^{*\pm}$ are forbidden. We consider the coupling assignment $f = -f'$ in our search for $\nu^* \rightarrow \nu\gamma$, and also for $\ell^{*\pm} \rightarrow \nu W^\pm$. With this coupling assignment, the photonic ν^* branching ratio varies from essentially 100% for ν^* masses less than the W^\pm mass to about 35% for masses of 160 GeV, and the branching ratio

¹In this paper, ℓ refers to any charged lepton, ℓ^\pm , or neutral lepton, ν .

for $\ell^{*\pm} \rightarrow \nu W^\pm$ varies from about 80% for $\ell^{*\pm}$ masses less than the W^\pm mass to about 65% for masses of 160 GeV. Again, the remaining $\ell^* \rightarrow \ell Z^0$ decays are not considered in this letter.

We search for pair production of charged excited leptons in the channels $e^+e^- \rightarrow \ell^{*+}\ell^{*-} \rightarrow \ell^+\ell^-\gamma\gamma$ (where $\ell^\pm = e, \mu$ or τ) and $e^+e^- \rightarrow \ell^{*+}\ell^{*-} \rightarrow \nu\bar{\nu}W^+W^-$, where the W^\pm are virtual in the excited lepton mass ranges accessible to this analysis. For the pair production of neutral excited leptons, we consider $e^+e^- \rightarrow \nu^*\bar{\nu}^* \rightarrow \ell^+\ell^-W^+W^-$ and $e^+e^- \rightarrow \nu^*\bar{\nu}^* \rightarrow \nu\bar{\nu}\gamma\gamma$. We search for the single production of charged excited leptons in $e^+e^- \rightarrow \ell^{*\pm}\ell^\mp \rightarrow \ell^+\ell^-\gamma$ and $e^+e^- \rightarrow \ell^{*\pm}\ell^\mp \rightarrow \nu\ell^\mp W^\pm$. Finally, for the single production of neutral excited leptons, we consider $e^+e^- \rightarrow \nu^*\nu \rightarrow \ell^\pm\nu W^\mp$ and $e^+e^- \rightarrow \nu^*\nu \rightarrow \nu\bar{\nu}\gamma$.

2 The OPAL Detector and Data Sample

A complete description of the OPAL detector can be found in Reference [9], and it is described only briefly here. The central detector consists of a system of tracking chambers that provides charged particle tracking over 96% of the full solid angle² inside a uniform 0.435 T magnetic field. It consists of a two layer silicon microstrip vertex detector, a high precision vertex drift chamber, a large volume jet chamber and a set of z chambers that measure the track coordinates along the beam direction. The ionization energy loss per unit path length in the jet chamber, dE/dx , is used for particle identification. A lead-glass electromagnetic calorimeter located outside the magnet coil covers the full azimuthal range with excellent hermeticity in the polar angle range of $|\cos\theta| < 0.82$ for the barrel region and $0.81 < |\cos\theta| < 0.984$ for the endcap region. The magnet return yoke is instrumented with streamer tubes with cathode strip readout for hadron calorimetry and consists of barrel and endcap sections along with pole tip detectors that together cover the region $|\cos\theta| < 0.99$. Muons are identified with the hadron calorimeter strips, and with four layers of muon chambers which cover the outside of the hadron calorimeter. The gamma catcher, forward detector and silicon tungsten electromagnetic calorimeters complete the geometrical acceptance down to 24 mrad. The silicon tungsten and forward detector calorimeters are used for the luminosity measurement.

The integrated luminosity used for this analysis is 10 pb^{-1} at $\sqrt{s} = 161.3 \text{ GeV}$. Backgrounds from different Standard Model processes are estimated with several event generators, described in the analysis sections of the paper. The background Monte Carlo samples generated have an equivalent integrated luminosity of at least six times that actually collected. All background and signal Monte Carlo samples are processed through the full OPAL detector simulation [10]. The background samples were generated, and the limits calculated, assuming $\sqrt{s} = 161.0 \text{ GeV}$.

3 Selection Criteria

In Section 3.1, we describe the search for the photonic decays of charged excited leptons in $\ell^+\ell^-\gamma\gamma$, $\ell^+\ell^-\gamma$, and $e\gamma$ topologies. Next, in Section 3.2 we describe the search for charged decays of charged and neutral excited leptons in $\ell^+\ell^-W^+W^-$, $\nu\bar{\nu}W^+W^-$ and $\nu\ell^\pm W^\mp$ topologies.

²The OPAL coordinate system is defined so that the z axis is in the direction of the electron beam and the x axis points towards the centre of the LEP ring; θ and ϕ are the polar and azimuthal angles, defined relative to the $+z$ - and $+x$ -axes, respectively.

Finally, in Section 3.3 we describe the search for the photonic decays of neutral excited leptons in events with purely photonic final states.

3.1 Charged Excited Leptons, Photonic Decays: $\ell^+\ell^-\gamma(\gamma)$ Topologies

The preselection, lepton and photon identification, and isolation requirements are identical to those used in Reference [3]. Briefly, we select low-multiplicity events, and identify tracks (or jets) as electron, muon or tau leptons using standard identification algorithms. Photons are identified as isolated electromagnetic calorimeter clusters, or as identified conversions. Simple kinematic constraints using the photon energy (energies) and the angles between the tau jets and the photon(s) are used to estimate the tau lepton energies.

Pair produced excited lepton candidate events with $\ell^+\ell^-\gamma\gamma$ final states are required to satisfy the following criteria:

1. There must be at least two identified leptons of the same flavour and at least two photons. The two most energetic leptons and two most energetic photons are used for further analysis. For the excited tau search, it is required that at most one of the two tau candidates also be an identified electron, and at most one also be an identified muon.
2. The sum of the energies of the two leptons and two photons, E_{tot} , must satisfy $1.6 E_{\text{beam}} < E_{\text{tot}} < 2.4 E_{\text{beam}}$, where E_{beam} is the beam energy.
3. With two leptons and two photons, there are two possible ways of forming the two lepton-photon mass combinations for each event. At least one of the two ways must have a difference between the mass combinations less than 10 GeV.

After all three cuts, no candidates are observed in the data for any channel, which is consistent with the expectation from Standard Model background sources. In the $e\gamma\gamma$ analysis, a total of 0.7 background events are expected, predominantly from radiative Bhabha scattering, which is modelled with the radiative e^+e^- event generator BHWIDE [11]. In the $\mu\mu\gamma\gamma$ analysis, a total of 0.3 background events are expected, predominantly from radiative muon pair production which is modelled with the radiative $\ell^+\ell^-$ event generator KORALZ [12]. In the $\tau\tau\gamma\gamma$ analysis, a total of 0.3 background events are expected, with contributions from radiative Bhabha scattering and from radiative tau pair production, which is modelled with KORALZ.

The efficiency for observing the pair production of excited leptons is evaluated at four selected masses from 65 GeV to 80 GeV at $\sqrt{s}=161$ GeV and is found to be independent of the centre-of-mass energy and of the excited lepton mass in the kinematic region of interest. The efficiency for observing the pair production of charged excited leptons with photonic decays is found to be about 57% for e^*e^* , 62% for $\mu^*\mu^*$ and 34% for $\tau^*\tau^*$.

Singly produced excited lepton candidate events with $\ell^+\ell^-\gamma$ final states are required to satisfy the following criteria:

1. There must be at least two identified leptons of the same flavour, at least one of which must have energy $E_\ell > 0.3 E_{\text{beam}}$, and exactly one photon with energy $E_\gamma > 0.3 E_{\text{beam}}$.

The two most energetic leptons and the photon are used for further analysis. For the excited tau search, it is required that at most one of the two tau candidates also be an identified electron, and at most one also be an identified muon.

2. The sum of the energies of the two leptons and one photon, E_{tot} , must satisfy $1.6 E_{\text{beam}} < E_{\text{tot}} < 2.4 E_{\text{beam}}$.
3. (a) For the e^* search, radiative Bhabha scattering is suppressed by requiring that the photon and at least one electron satisfy $|\cos \theta| < 0.7$.
 (b) For the τ^* search, radiative Bhabha scattering and muon pair events with an unidentified lepton are suppressed by requiring that the energy sum of the 2 jets corresponding to the tau candidates and the one photon satisfy $E_{\text{jet},1} + E_{\text{jet},2} + E_\gamma < 1.8 E_{\text{beam}}$.
4. The process $e^+e^- \rightarrow Z\gamma \rightarrow \ell^+\ell^-\gamma$ is suppressed by vetoing events with $75 \text{ GeV} < M_{\ell\ell} < 105 \text{ GeV}$, where $M_{\ell\ell}$ is the invariant mass of the lepton pair.

After all cuts, four events are observed in the $ee\gamma$ analysis, no events in the $\mu\mu\gamma$ analysis, and one event in the $\tau\tau\gamma$ analysis. With two leptons and one photon, there are two possible lepton-photon mass combinations for each event. The $\ell^\pm\gamma$ invariant mass distributions for both combinations are plotted in Figures 1(a), (c) and (d) for e^* , μ^* and τ^* , respectively. In the $ee\gamma$ analysis, a total of 4.1 background events is expected. The dominant background is from radiative Bhabha scattering, evaluated with BHWIDE. In the $\mu\mu\gamma$ analysis, a total of 3.0 background events is expected. The dominant background is from radiative muon pair events, evaluated with KORALZ. In the $\tau\tau\gamma$ analysis, a total of 2.3 background events is expected. The dominant background is from radiative tau pair events, evaluated with KORALZ. The deficit in the muon and tau channels appears only after the final analysis cut, and all prior kinematic distributions appear well modelled by the Monte Carlo generators.

If the $e^*\epsilon\gamma$ coupling is non-negligible, the single production of excited electrons is dominated by t -channel photon exchange. A significant fraction of singly produced e^* events would then have the recoil electron at a small polar angle outside the detector acceptance, making the search for the $e\gamma$ final state also desirable. For the $e\gamma$ final state analysis, the energy and direction of the missing electron are inferred using conservation of momentum from the observed electron and photon by assuming an $ee\gamma$ topology.

Candidate $e\gamma$ events are required to satisfy the following criteria:

1. There must be exactly one identified electron with energy $E_e > 0.3 E_{\text{beam}}$ and exactly one photon with energy $E_\gamma > 0.3 E_{\text{beam}}$.
2. The energy sum of the observed e^\pm , the inferred missing e^\mp , and the photon, E_{tot} , must satisfy $1.6 E_{\text{beam}} < E_{\text{tot}} < 2.4 E_{\text{beam}}$.
3. Bhabha scattering is suppressed by requiring the photon to satisfy $|\cos \theta_\gamma| < 0.7$, and that the event thrust axis formed with the observed lepton and photon satisfy $|\cos \theta_{\text{thrust}}| < 0.9$.
4. Events which pass the above $ee\gamma$ selection are removed, making the two analyses orthogonal.

After all cuts, 28 events are observed in the $e\gamma$ analysis. A total of 31.9 background events is expected. The dominant background for this topology is from t -channel radiative Bhabha scattering with one electron missing along the beam axis, evaluated with the radiative e^+e^- event generator TEEGG [13]. The number of observed events is compatible with the expectation from Standard Model sources. The $e\gamma$ invariant mass distribution for this topology is plotted in Figure 1(b). No peak is observed.

The number of events observed in each channel is compatible with that expected from Standard Model sources, and no anomalous structure is apparent in the lepton-photon mass distributions. We conclude that there is no evidence for excited lepton production in these topologies.

When computing limits for an excited lepton with mass M_* , all events with at least one lepton-photon mass combination, $M_{\ell\gamma}$, satisfying $|M_{\ell\gamma} - M_*| < \Delta$ were considered signal candidates. The mass half-window, Δ , is 4 GeV, 8 GeV and 8 GeV for e^* , μ^* and τ^* , respectively. The values chosen for Δ are about 2σ of the mass resolution estimated from Monte Carlo. For the excited electron search, events which pass either the $e\gamma$ or $ee\gamma$ selections are considered as signal candidates. The efficiency for observing the single production of excited leptons with photonic decays was evaluated for four selected masses between 80 GeV and 155 GeV at $\sqrt{s} = 161$ GeV. The efficiency at an arbitrary mass is estimated from the linear interpolation between two of these points. The efficiency varies from 35% at a mass of 80 GeV to 54% at a mass of 155 GeV for e^* , from 45% to 66% for μ^* and from 25% to 30% for τ^* .

3.2 Charged and Neutral Excited Leptons, Charged Decays: $\ell\bar{\ell}W^+W^-$, $\nu\bar{\nu}W^+W^-$ and $\nu\ell^\pm W^\mp$ Topologies

The search for charged decays of pair produced excited leptons uses the same analysis as the search for the production of unstable heavy leptons (L^0 and L^\pm) with ‘‘flavour mixing’’ decays described in Reference [14]. The topologies $e^+e^- \rightarrow L^0\bar{L}^0 \rightarrow \ell^+\ell^-W^+W^-$ and $e^+e^- \rightarrow L^+L^- \rightarrow \nu\bar{\nu}W^+W^-$ are almost identical to neutral and charged excited lepton pair production with charged decays, respectively. No events are observed in that analysis. The total selection efficiency for charged decays of pair produced excited leptons at $\sqrt{s} = 161$ GeV is evaluated at four selected masses from 65 GeV to 80 GeV, and is found to be about 38% for ν_e^* , 45% for ν_μ^* , 25% for ν_τ^* and 22% for each $\ell^{*\pm}$ flavour.

Two searches are performed for the charged decays of singly produced excited leptons. The first analysis looks only for leptonic decays of the W^\pm , which may be real or virtual depending on the mass of the ν^* . The topology is then $e^+e^- \rightarrow \nu_\ell^*\nu_\ell \rightarrow \nu_\ell\ell^\pm W^\mp \rightarrow \nu_\ell\ell^\pm\nu_\ell\ell'^\mp$, where ℓ^\pm corresponds to the excited lepton flavour, and ℓ'^\mp may or may not be of the same flavour. Since charged excited leptons with charged decays, $e^+e^- \rightarrow \ell^{*\pm}\ell^\mp \rightarrow \nu_\ell\ell^\pm W^\mp \rightarrow \nu_\ell\ell^\pm\nu_\ell\ell'^\mp$, can have the same final states as neutral excited leptons with charged decays, the same search is used. The topology is a pair of leptons which are not coplanar with the beam direction.

Using the same preselection and track quality cuts as the $\ell^+\ell^-\gamma(\gamma)$ analysis in Section 3.1 and described in Reference [3], candidate $\ell^{*\pm}$ and ν_ℓ^* events are required to satisfy the following criteria:

1. There must be two identified leptons, at least one of type ℓ^\pm corresponding to the excited lepton flavour. At least one of the leptons must have an energy greater than $0.2 E_{\text{beam}}$.

The lepton identification criteria are the same as those used in Section 3.1 and Reference [3].

2. There must be no other track passing the quality cuts in the event.
3. Excluding the clusters associated with the two leptons, the sum of other barrel and endcap electromagnetic calorimeter cluster energies must be less than 10 GeV.
4. Events from two-photon processes are suppressed by requiring that there is no significant energy in either side of the forward detector (less than 2 GeV), silicon tungsten (less than 5 GeV), or gamma catcher (less than 5 GeV) electromagnetic calorimeters.
5. Events with missing momentum along the beam axis are removed by requiring $|\cos \theta_{\text{miss}}| < 0.9$, where θ_{miss} is the polar angle of the missing momentum.
6. Events are required to be acoplanar by requiring $\phi_{\ell\ell}^{\text{ACOP}} > 20^\circ$ ($\phi_{\ell\ell}^{\text{ACOP}}$ is 180° minus the opening angle between the two leptons in the x - y plane).

After all cuts, one event is observed with 1.8 background events expected in the $e\ell^\pm$ topology, one event observed with 1.7 background events expected in the $\mu\ell^\pm$ topology and three events observed with 2.7 background events expected in the $\tau\ell^\pm$ topology. The dominant background is from 4-fermion production, evaluated with the grc4f event generator [15]. This background is also evaluated with EXCALIBUR [16], which gives consistent background estimates.

The second search for the charged decays of singly produced excited leptons is optimised for the hadronic decays of the W^\pm boson, looking in the $e^+e^- \rightarrow \nu_\ell^* \nu_\ell \rightarrow \nu_\ell \ell^\pm W^\mp \rightarrow \nu_\ell \ell^\pm q\bar{q}'$ channels. In this search, we look only in the electron and muon channels; the high background levels in the tau channel do not allow the sensitivity of the preceding acoplanar lepton pair analysis to be improved. Since charged excited leptons with charged decays, $e^+e^- \rightarrow \ell^{*\pm} \ell^\mp \rightarrow \nu_\ell \ell^\pm W^\mp \rightarrow \nu_\ell \ell^\pm q\bar{q}'$, can have the same final states as neutral excited leptons with charged decays, the same search is used.

Charged particle tracks are required to satisfy the same quality cuts used in [17]. A preselection is also performed: the number of charged tracks is required to be at least six, and the ratio of the number of tracks passing the quality cuts to the total number of charged tracks is required to be larger than 0.2. Candidate ℓ^* and ν_ℓ^* events are then required to satisfy the following criteria:

1. There must be at least one isolated lepton ℓ^\pm ($\ell^\pm = e$ or μ), corresponding to the excited lepton flavour, using the following criteria.

Electrons are identified using their dE/dx and their energy deposition in the electromagnetic calorimeters, as described in References [18] and [19] for the barrel and endcap regions, respectively. Muons are identified by matching track segments in the muon chambers with tracks in the central detector [20]. In the region not covered by the muon chambers, muons are identified using the hadron calorimeter strips [18]. Charged tracks are considered isolated if there are no additional tracks in a 15° half-opening angle cone centred on the track. The momentum of a lepton candidate is required to be larger than 2 GeV.

If there is more than one isolated lepton corresponding to the considered lepton flavour, the highest energy lepton is used in the following selection.

2. Events from two-photon processes and $e^+e^- \rightarrow qq(\gamma)$ are reduced by requiring that there is no significant energy in either side of the forward detector (less than 2 GeV), silicon tungsten (less than 5 GeV), or gamma catcher (5 GeV) electromagnetic calorimeters.
3. Events from two-photon processes are further reduced by requiring that R_{vis} , the visible energy normalized to \sqrt{s} , is greater than 0.3.
4. Events with energy missing along the beam axis are removed by requiring $|\cos \theta_{\text{miss}}| < 0.9$.
5. $e^+e^- \rightarrow qq(\gamma)$ events are further reduced by requiring that the thrust value is less than 0.95.
6. Events are required to have a large missing transverse momentum (p_t^{miss}) or a large lepton momentum (p_ℓ) by requiring that $(p_t^{\text{miss}} + p_\ell)/E_{\text{beam}} > 0.4$.
7. A kinematic fit is performed to reduce the W-pair and residual $e^+e^- \rightarrow qq(\gamma)$ background. Removing the isolated lepton from the event, the rest of the event is forced into two jets using the Durham jet-finding algorithm [21]. The measured parameters of the lepton, the missing momentum, and the two jets are used as input to a kinematic fit, which imposes conservation of energy and momentum. From the fit results, the invariant mass of the lepton plus missing energy, $M_{\ell\text{-miss}}$, and the jet pair, $M_{j\text{-}j}$, are extracted, and the following cuts are made:
 - $M_{\ell\text{-miss}} > 5 \text{ GeV}$ and $M_{j\text{-}j} < 95 \text{ GeV}$.
 - $M_{\ell\text{-miss}} + M_{j\text{-}j} < 145 \text{ GeV}$.

The fitted masses $M_{\ell\text{-miss}}$ vs. $M_{j\text{-}j}$ are plotted in Figure 2 immediately before cut 7 for data, background and signal Monte Carlo. After all cuts, two events are observed with 0.6 background events expected in the eqq' channel and no events are observed with 0.9 background events expected in the $\mu qq'$ channel. The dominant background is from 4-fermion production, evaluated EXCALIBUR and cross-checked with grc4f.

The number of events observed in each channel is compatible with that expected from Standard Model sources, and we conclude that there is no evidence for excited lepton production in these topologies. When computing limits, events which pass either the acoplanar lepton pair or $\ell^\pm qq'$ selection for the muon or electron topologies are considered as signal candidates. The efficiency for observing the single production of excited leptons with charged decays is about 50% for ν_e^* , ν_μ^* , e^* and μ^* , and about 15% for ν_τ^* and τ^* . There is a small dependence on the ℓ^* mass, which is taken into account in the results.

3.3 Neutral Excited Lepton, Photonic Decays: $\nu\bar{\nu}\gamma\gamma$ and $\nu\bar{\nu}\gamma$ Topologies

The OPAL analysis of photonic final states [6] includes two missing energy topologies:

Topology A: One or two photons accompanied by invisible particle(s) ($e^+e^- \rightarrow \gamma(\gamma) + \text{invisible particle(s)}$). At least one photon with $E_\gamma > 0.2 E_{\text{beam}}$ and $|\cos \theta| < 0.7$ is required.

Topology B: Acoplanar photon pair ($e^+e^- \rightarrow \gamma\gamma + \text{invisible particle(s)}$). Two photons each with energy exceeding 1.75 GeV and $|\cos\theta| < 0.7$ are required.

This analysis, described in detail in Reference [6] for the analysis of data taken at $\sqrt{s} = 130$ and 136 GeV, is also applied to the $\sqrt{s} = 161$ GeV sample.

Topology B is used for the search for pair production in the channel $e^+e^- \rightarrow \nu^*\bar{\nu}^* \rightarrow \nu\bar{\nu}\gamma\gamma$. After the standard Topology B selection, a background of 0.96 events is expected, which is reduced with further cuts. The primary background from $e^+e^- \rightarrow \nu\bar{\nu}\gamma\gamma$ is evaluated with the event generator NUNUGPV [22]. The background from $e^+e^- \rightarrow Z^0\gamma\gamma \rightarrow \nu\bar{\nu}\gamma\gamma$ is reduced by requiring that the sum of the two photon energies be greater than $0.4\sqrt{s}$. No events are observed with a total expected background is 0.04 events, and the efficiency for observing the pair production of excited neutrinos with photonic decays is about 30%.

Topology A is used for the search for single production in the channel $e^+e^- \rightarrow \nu^*\nu \rightarrow \nu\bar{\nu}\gamma$. After the standard Topology A selection, 10 events are observed with an expected background of 14.2 event, which is reduced with further cuts. The primary background from $e^+e^- \rightarrow \nu\bar{\nu}\gamma$ is evaluated with NUNUGPV. The background from $e^+e^- \rightarrow Z^0\gamma \rightarrow \nu\bar{\nu}\gamma$ is reduced by requiring that there is only one photon with $E_\gamma > 0.2 E_{\text{beam}}$, and that the missing mass in the event, M_{miss} , satisfies $M_{\text{miss}} < 75$ GeV. With these requirements, no events are observed in the data with a total expected background of 0.04 events, and the efficiency for observing the single production of excited neutrinos with photonic decays varies from about 16% at a mass of 80 GeV to 53% at a mass of 155 GeV.

4 Results

The systematic errors in the total number of expected signal events are estimated from: the statistical error on the Monte Carlo estimate of the detection efficiency (typically 1%), including an additional error (5%) for the interpolation between excited lepton mass points; the error on the integrated luminosity (0.6%); uncertainties in the modelling of the particle identification cuts (2.5% if one identified lepton is required, 5% if two are required); uncertainties in the modelling of the photon conversion finder used in the $\ell^+\ell^-\gamma(\gamma)$ analyses (1% per photon in the event). The errors are considered to be independent and are added in quadrature for the total systematic error, which is typically about 7%. The systematic error is incorporated into the limits using the method described in Reference [23]. Background subtraction is not performed in any of the limits calculated with these data.

The production cross-sections from Reference [8] (corrected for the effects of initial state radiation [24]), branching ratios from References [8] and [25], and measured efficiencies are used to calculate the number of events expected for an excited lepton of a given mass. Poisson statistics for the number of observed events are used to set limits on the maximum number of events in each analysis.

Limits on the excited lepton masses are inferred from the pair production searches. The 95% confidence level lower mass limits are listed in Table 1, along with the coupling assumptions which are used for the branching ratio calculation for each topology.

Limits on the ratio of the coupling to the compositeness scale, f/Λ , are inferred from the single production searches. Limits on f/Λ for charged excited leptons with $f = f'$ from the

Flavour	Decays	Coupling	Mass Limit $\sqrt{s} = 161$ GeV (GeV)
e^*	Photonic	$f = f'$	79.9
μ^*	Photonic	$f = f'$	80.0
τ^*	Photonic	$f = f'$	79.1
e^*	Charged	$f = -f'$	77.1
μ^*	Charged	$f = -f'$	77.1
τ^*	Charged	$f = -f'$	77.1
ν_e^*	Charged	$f = f'$	78.3
ν_μ^*	Charged	$f = f'$	78.9
ν_τ^*	Charged	$f = f'$	76.2
ν_e^*	Photonic	$f = -f'$	77.8
ν_μ^*	Photonic	$f = -f'$	77.8
ν_τ^*	Photonic	$f = -f'$	77.8

Table 1: 95% confidence level lower mass limits for the different excited leptons from the pair creation searches. The coupling assumption is necessary for the branching ratio calculation.

photonic decay mode search are plotted in Figure 3(a), for charged excited leptons with $f = -f'$ from the W^\pm decay mode search in Figure 3(b), for neutral excited leptons with $f = f'$ from the W^\pm decay mode search in Figure 3(c), and for neutral excited leptons with $f = -f'$ from the γ decay mode search in Figure 3(d).

5 Conclusion

We have analysed a data sample with an integrated luminosity of 10 pb^{-1} at 161 GeV, collected with the OPAL detector at LEP, to search for the production of excited leptons. No evidence for excited leptons was found, and limits on masses and couplings are established within the framework of the model described in Reference [8]. From the search for pair production, lower mass limits are established. From the search for single production, upper limits on the ratio of the coupling to the compositeness scale are established. These limits substantially improve those from previous LEP searches [3, 4].

6 Acknowledgements

We particularly wish to thank the SL Division for the efficient operation of the LEP accelerator at the new energy of $\sqrt{s} = 161$ GeV and for their continuing close cooperation with our experimental group. We thank our colleagues from CEA, DAPNIA/SPP, CE-Saclay for their efforts over the years on the time-of-flight and trigger systems which we continue to use. In addition to the support staff at our own institutions we are pleased to acknowledge the Department of Energy, USA, National Science Foundation, USA,

Particle Physics and Astronomy Research Council, UK,
Natural Sciences and Engineering Research Council, Canada,
Israel Science Foundation, administered by the Israel Academy of Science and Humanities,
Minerva Gesellschaft,
Japanese Ministry of Education, Science and Culture (the Monbusho) and a grant under the
Monbusho International Science Research Program,
German Israeli Bi-national Science Foundation (GIF),
Bundesministerium für Bildung, Wissenschaft, Forschung und Technologie, Germany,
National Research Council of Canada,
Hungarian Foundation for Scientific Research, OTKA T-016660, and OTKA F-015089.

References

- [1] OPAL Collaboration, M. Z. Akrawy *et al.*, Phys. Lett. B 257 (1990) 531.
- [2] ALEPH Collaboration, D. Decamp *et al.*, Phys. Lett. B 250 (1990) 172;
DELPHI Collaboration, P. Abreu *et al.*, Z. Phys. C53 (1992) 41;
L3 Collaboration, M. Acciarri *et al.*, Phys. Lett. B 353 (1995) 136.
- [3] OPAL Collaboration, G. Alexander *et al.*, “Search for Excited Leptons in e^+e^- Collisions at $\sqrt{s} = 130$ and 136 GeV,” CERN-PPE/96-094, to be published in Phys. Lett. B. (1996).
- [4] L3 Collaboration, M. Acciarri *et al.*, Phys. Lett. B 370 (1996) 211;
DELPHI Collaboration, P. Abreu *et al.*, Phys. Lett. B 380 (1996) 480;
ALEPH Collaboration, D. Buskulic *et al.*, “Search for Excited Leptons at 130 - 140 GeV,” CERN-PPE/96-087, submitted to Phys. Lett. B.
- [5] H1 Collaboration, I. Abt *et al.*, Nucl. Phys. B 396 (1993) 3;
ZEUS Collaboration, M. Derrick *et al.*, Z. Phys. C65 (1994) 627.
- [6] OPAL Collaboration, G. Alexander *et al.*, Phys. Lett. B377 (1996) 222.
- [7] L3 Collaboration, M. Acciarri *et al.*, Phys. Lett. B 353 (1995) 136;
ALEPH Collaboration, D. Buskulic *et al.*, “A study of single and multi-photon production in e^+e^- collisions at centre-of-mass energies of 130 and 136 GeV,” CERN-PPE/96-53 (1996), submitted to Phys. Lett. B.
- [8] F. Boudjema, A. Djouadi, J. L. Kneur, Z. Phys. C57 (1993) 425.
- [9] OPAL Collaboration, K. Ahmet *et al.*, Nucl. Instr. Meth. A 305 (1991) 275;
P. P. Allport *et al.*, Nucl. Instr. Meth. A 324 (1993) 34;
P. P. Allport *et al.*, Nucl. Instr. Meth. A 346 (1994) 476;
B. E. Anderson *et al.*, IEEE Trans. Nucl. Sci. 41 (1994) 845.
- [10] J. Allison *et al.*, Nucl. Instr. Meth. A 317 (1992) 47.
- [11] S. Jadach, W. Placzek and B. F. L. Ward, University of Tennessee preprint, UTHEP 95-1001 (unpublished).

- [12] S. Jadach, B. F. L. Ward and Z. Wąs, *Comp. Phys. Comm.* 79 (1994) 503.
- [13] D. Karlen, *Nucl. Phys. B* 289 (1987) 23.
- [14] OPAL Collaboration, G. Alexander *et al.*, “Search for Unstable Heavy Leptons in e^+e^- Collisions at Centre-of-Mass Energies of 161 GeV,” CERN-PPE/96-xxx (1996), to be submitted to *Phys. Lett. B*.
- [15] J. Fujimoto *et al.*, KEK preprint KEK-CP-046, (1996).
- [16] F.A. Berends, R. Pittau and R. Kleiss, *Comp. Phys. Comm.* 85 (1995) 437.
- [17] OPAL Collaboration, G. Alexander *et al.*, *Phys. Lett. B*377 (1996) 181;
OPAL Collaboration, G. Alexander *et al.*, *Phys. Lett. B*377 (1996) 273.
- [18] OPAL Collaboration, R. Akers *et al.*, *Z. Phys. C*60 (1993) 199.
- [19] OPAL Collaboration, R. Akers *et al.*, *Z. Phys. C*60 (1993) 19.
- [20] OPAL Collaboration, P. Acton *et al.*, *Z. Phys. C*58 (1993) 523.
- [21] N. Brown and W. J. Stirling, *Phys. Lett. B*252 (1990) 657;
S. Bethke, Z. Kunszt, D. Soper and W. J. Stirling, *Nucl. Phys. B*370 (1992) 310;
S. Catani *et al.*, *Nucl. Phys. B*269 (1991) 432;
N. Brown and W. J. Stirling, *Z. Phys. C*53 (1992) 629.
- [22] G. Montagna *et al.*, *Nucl. Phys. B*452 (1995) 161.
- [23] R. D. Cousins and V. L. Highland, *Nucl. Instr. Meth. A* 320 (1992) 331.
- [24] The initial state radiation is implemented according to the formulae in F. A. Berends, R. Pittau and R. Kleiss, *Nucl. Phys. B* 426 (1994) 344.
- [25] F. Boudjema and A. Djouadi, *Phys. Lett. B* 240 (1990) 485.

OPAL

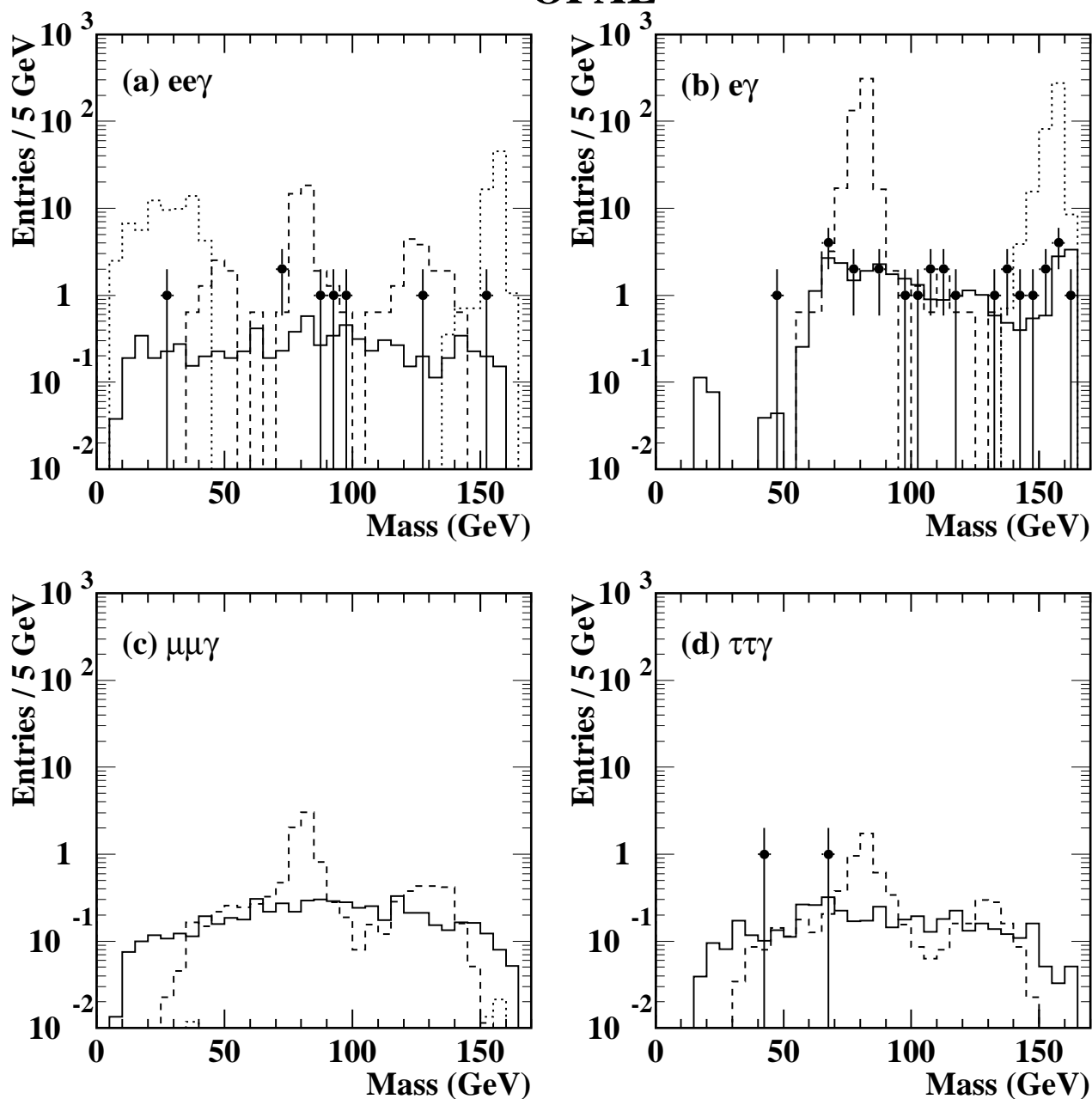


Figure 1: Lepton-photon invariant mass distribution after all cuts in the search for the single production of charged excited leptons with photonic decays. (a) is for e^* with two visible final state electrons, (b) is for e^* with one visible final state electron, (c) is for μ^* (no observed candidates) and (d) is for τ^* . The dashed and dotted lines are signal Monte Carlo with $f/\Lambda = (200 \text{ GeV})^{-1}$ and with $\ell^{*\pm}$ masses of 80 and 155 GeV, respectively, the solid lines are the sum of all of the Standard Model background Monte Carlos and the filled circles are the full data set. In (a), (c) and (d), both mass combinations are plotted for each event.

OPAL

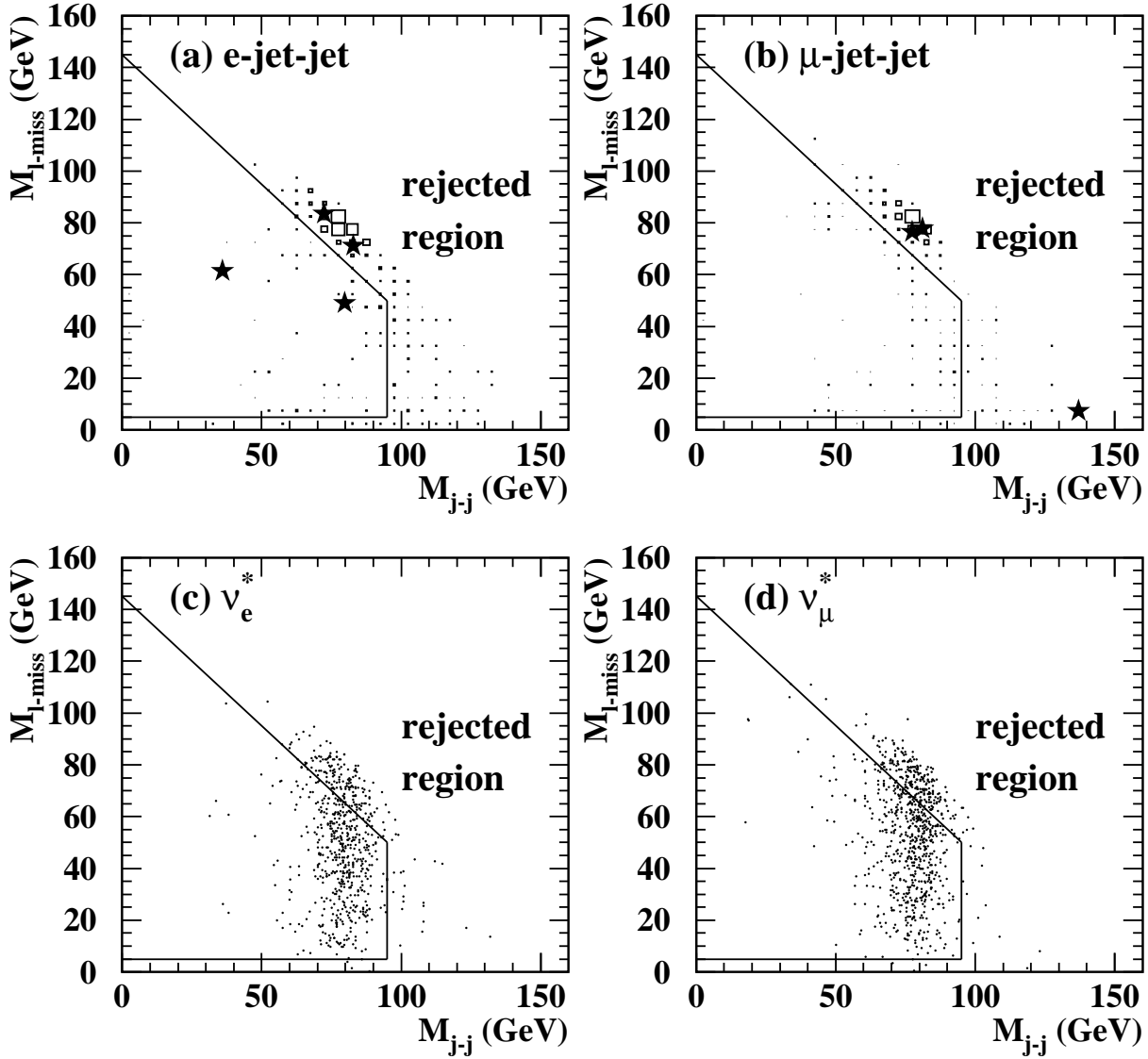


Figure 2: $M_{\ell-miss}$ vs. M_{j-j} after all other cuts in the search for the single production of excited leptons with charged decays. (a) and (b) are for the electron and muon channels, respectively, for real data (stars) and background Monte Carlo (boxes). (c) and (d) are for ν_e^* and ν_μ^* , respectively, for excited lepton masses of 120 GeV. Each signal Monte Carlo sample corresponds to 2000 generated events. The signal and background Monte Carlo are not normalized to the integrated luminosity. The cut is shown as the solid line.

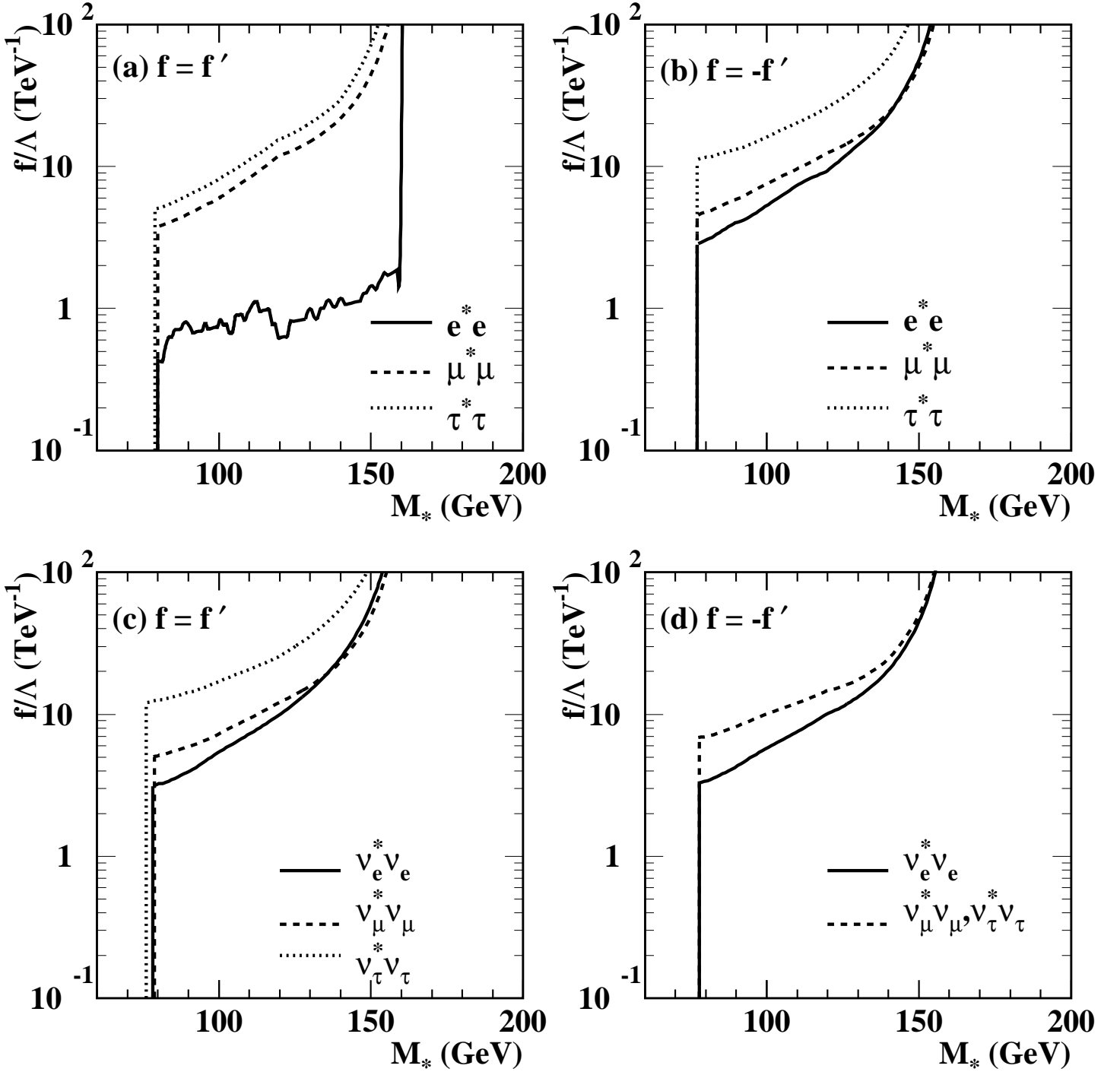


Figure 3: 95% confidence level upper limits on the ratio of the the coupling to the compositeness scale, f/Λ , as a function of the excited lepton mass. (a) shows the limits on e^* , μ^* and τ^* with $f = f'$, (b) shows the limits on e^* , μ^* and τ^* with $f = -f'$, (c) shows the limits on ν_e^* , ν_μ^* and ν_τ^* with $f = f'$, and (d) shows the limits on ν_e^* , ν_μ^* and ν_τ^* with $f = -f'$. The structure of the limits on e^* in (a) correspond to the events which pass the full selection, as described in the text. The regions above and to the left of the curves are excluded by the single and pair production searches, respectively.